

Image-Based Annotation of Chemogenomic Libraries for Phenotypic Screening

Amelie Tjaden ^{1,2}, Apirat Chaikuad ^{1,2}, Eric Kowarz ³, Rolf Marschalek ³, Stefan Knapp ^{1,2}, Martin Schröder ^{1,2,*} and Susanne Müller ^{1,2,*}

- ¹ Institute of Pharmaceutical Chemistry, Goethe University Frankfurt, Max-von-Laue-Str.9, 60438 Frankfurt, Germany; tjaden@pharmchem.uni-frankfurt.de (A.T.); chaikuad@pharmchem.uni-frankfurt.de (A.C.); knapp@pharmchem.uni-frankfurt.de (S.K.)
 - ² Structural Genomics Consortium, BMLS, Goethe University Frankfurt, Max-von-Laue-Str. 15, 60438 Frankfurt, Germany
 - ³ Institute of Pharmaceutical Biology, Goethe University, Max-von-Laue-Str.9, 60438 Frankfurt, Germany; kowarz@em.uni-frankfurt.de (E.K.); rolf.marschalek@em.uni-frankfurt.de (R.M.)
- * Correspondence: m.schroeder@pharmchem.uni-frankfurt.de (M.S.); susanne.mueller-knapp@bmls.de (S.M.)

Table of contents

Supplementary Figure S1: Hoechst33342 dye titration in HeLa cells after 20 h.

Supplementary Figure S2. Analysis of Cell Nuclei by Hoechst Channel Intensity level

Supplementary Figure S3: Fluorescence Spectrum of berzosertib

Supplementary Figure S4: Validation of Multiplex high Via protocol

Supplementary Figure S5: Hoechst High Intensity Object

Supplementary Figure S6: Viability analysis over nuclei gating protocol

Supplementary Figure S7: Phenotypical property analysis in HEK293T cells

Supplementary Figure S8: Phenotypical property analysis in MRC-9 cells

Supplementary Figure S9: Spectra Viewer visualization

Supplementary Table S1: Concentrations in μM of tested cell staining dyes

Supplementary Table S2: reference compounds tested in High-Via Extend protocol

Supplementary Table S3: Compounds tested in FUCCI Assay System

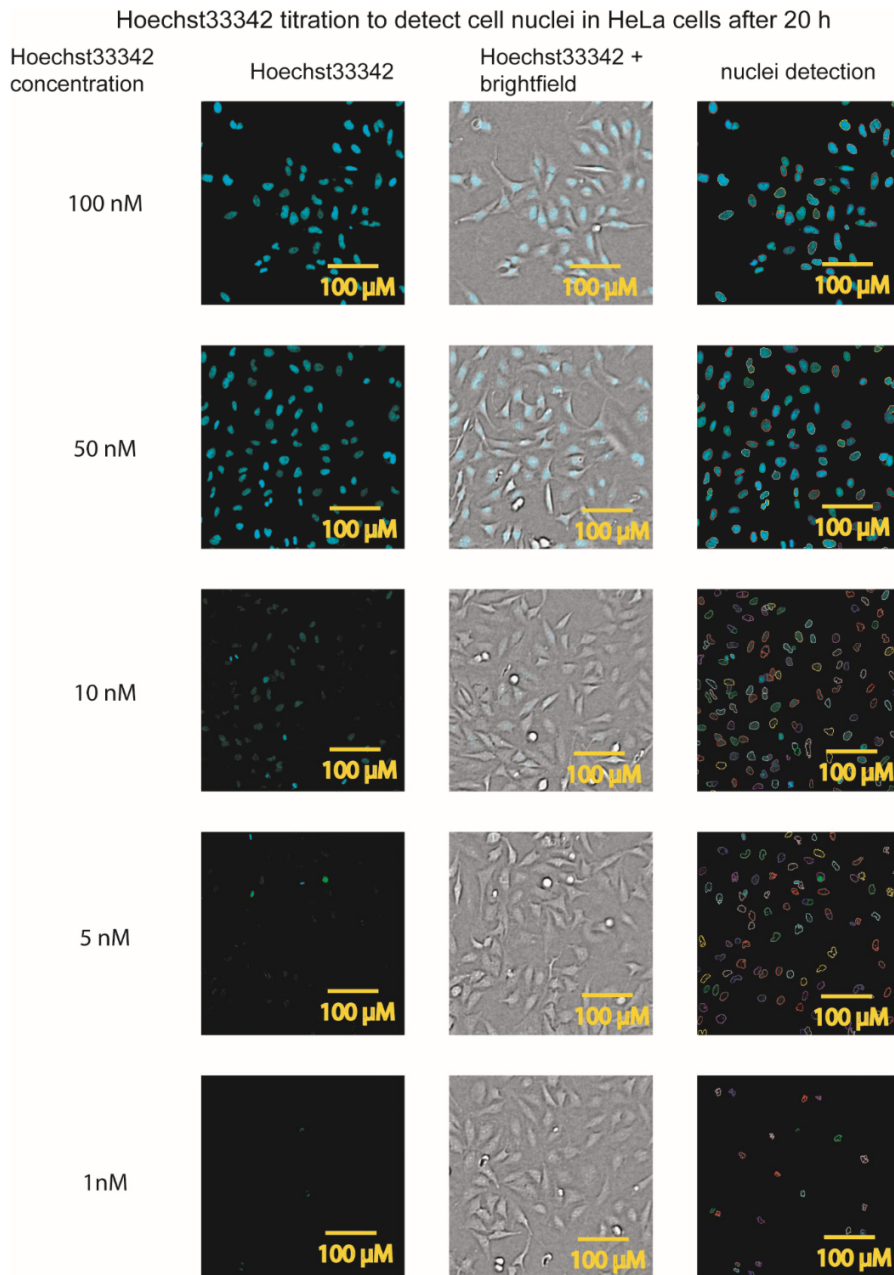
Supplementary Table S4: Additional data FUCCI assay (Excel)

Supplementary Table S5: References used for Multiplex protocol

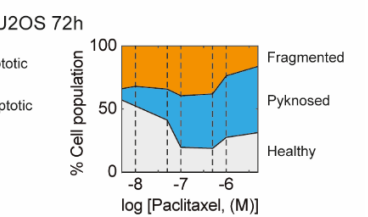
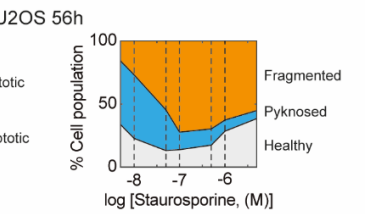
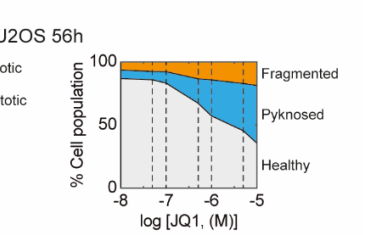
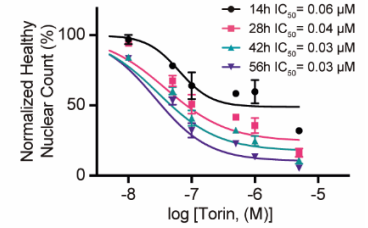
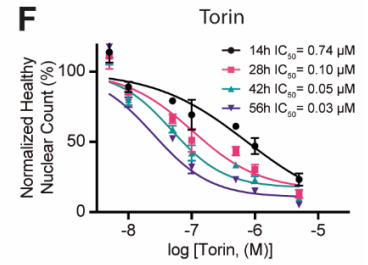
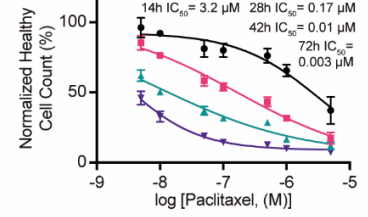
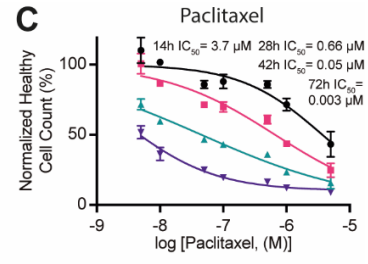
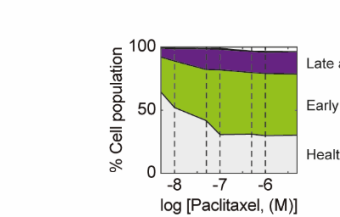
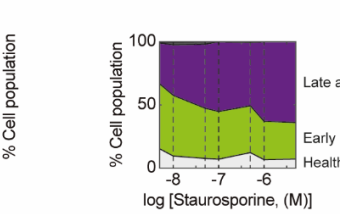
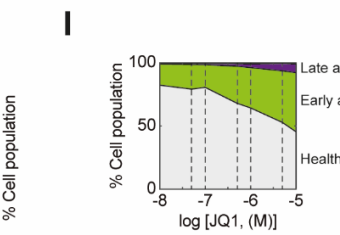
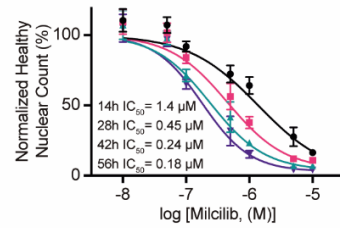
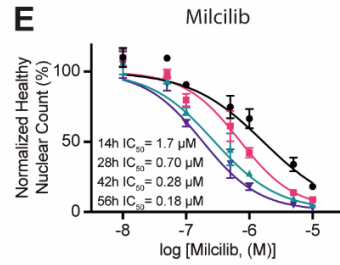
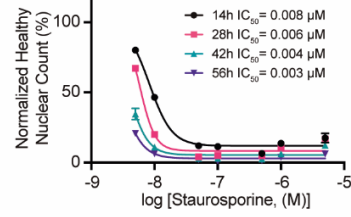
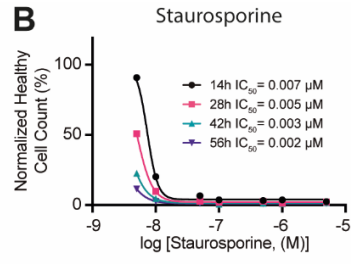
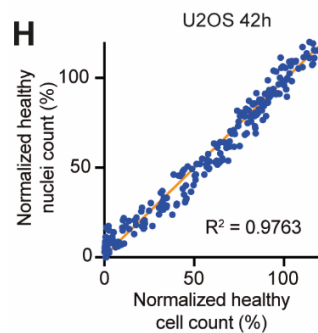
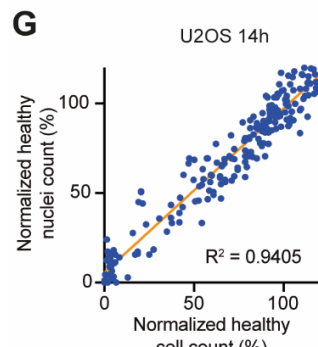
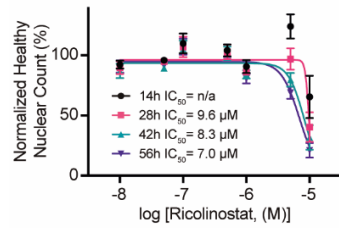
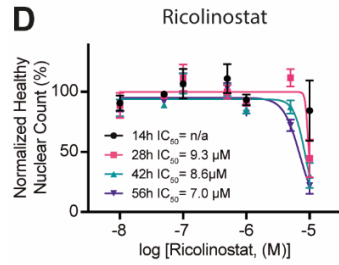
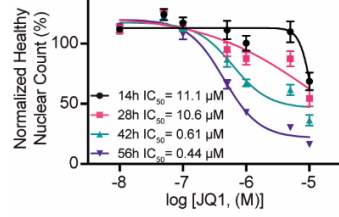
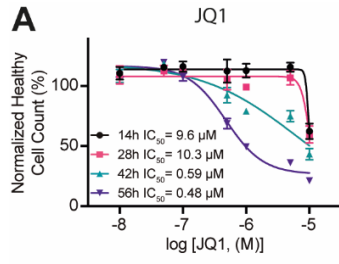
Supplementary Table S6: Trainings set

Supplementary Table S7: Features of machine learning algorithm

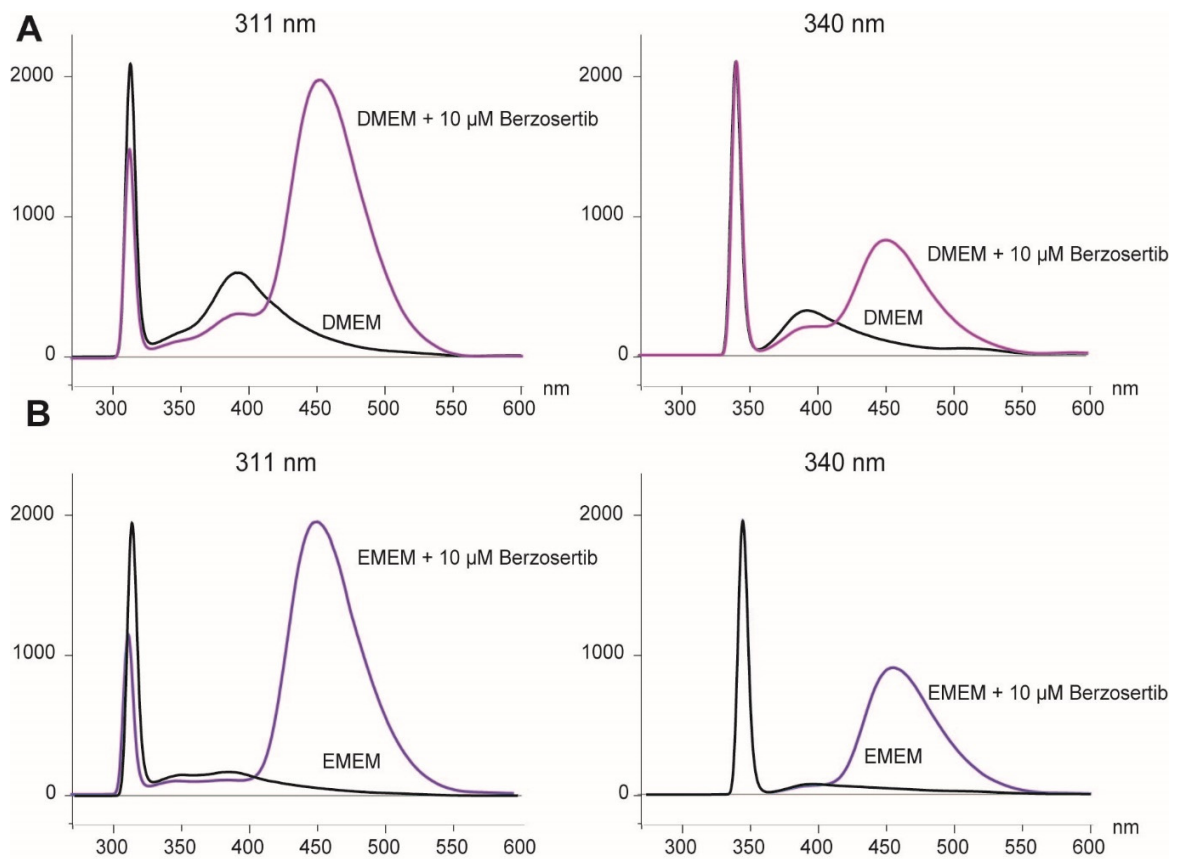
Supplementary Table S8: Multiplex Chemogenomic data (Excel)



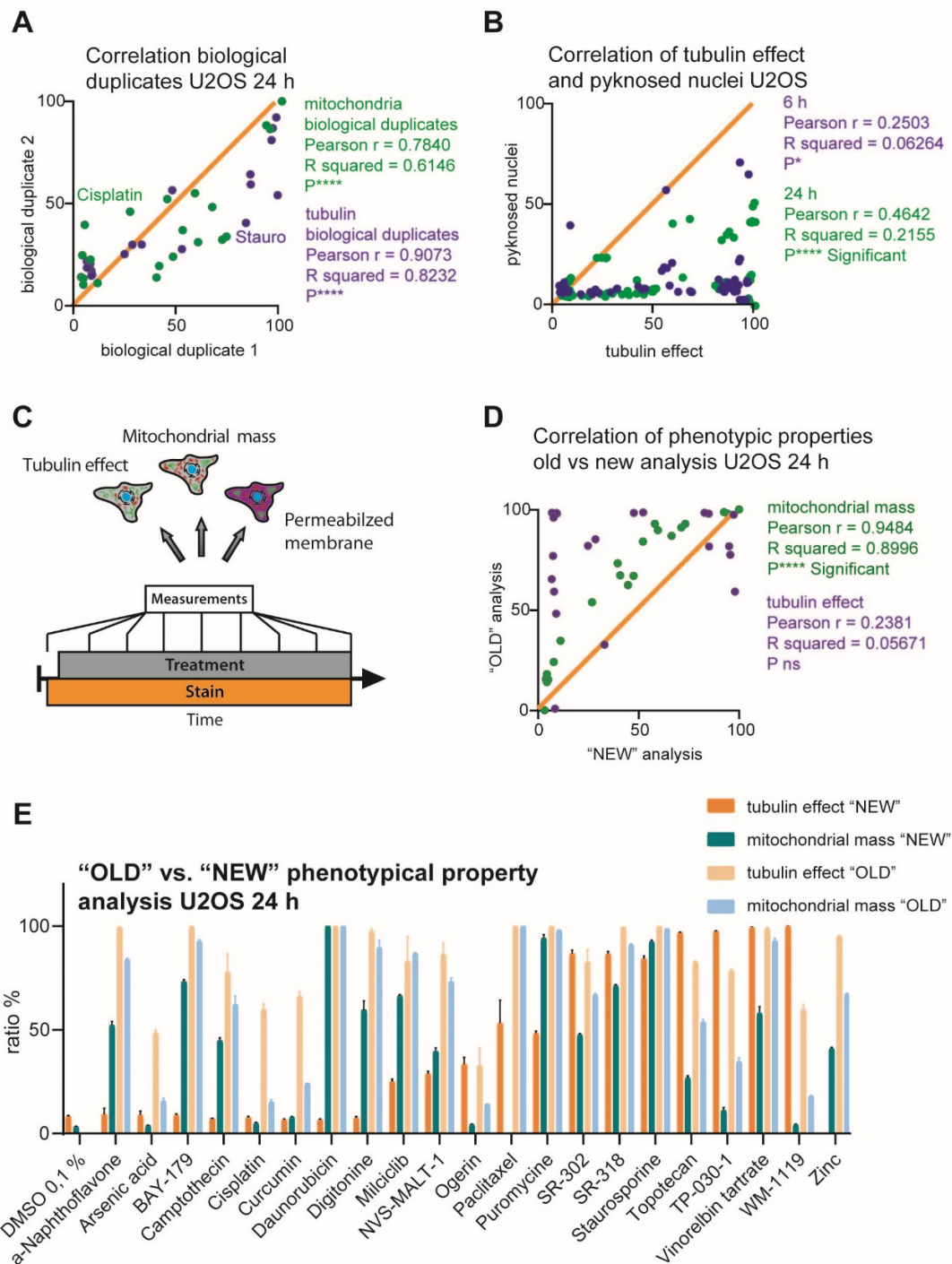
Supplementary Figure S1: Hoechst33342 dye titration in HeLa cells after 20 h. Fluorescence images, bright field images and nuclei detection of HeLa cells, after 20 h of exposure to different concentrations of Hoechst33342 stain (100 nM, 50 nM, 10 nM, 5 nM, 1 nM).



Supplementary Figure S2. Analysis of Cell Nuclei by Hoechst Channel Intensity level A Normalized healthy cell count and normalized healthy nuclear count of different concentrations (0.01 μM , 0.05 μM , 0.1 μM , 0.5 μM , 1 μM , 5 μM , 10 μM) of JQ1 exposure with calculated IC50 values after 14h, 28h, 42h and 56h. **B** Normalized healthy cell count and normalized healthy nuclear count of different concentrations (0.01 μM , 0.05 μM , 0.1 μM , 0.5 μM , 1 μM , 5 μM , 10 μM) of staurosporine exposure with calculated IC50 values after 14h, 28h, 42h and 56h. **C** Normalized healthy cell count and normalized healthy nuclear count of different concentrations (0.01 μM , 0.05 μM , 0.1 μM , 0.5 μM , 1 μM , 5 μM , 10 μM) of paclitaxel exposure with calculated IC50 values after 14h, 28h, 42h and 56h. **D** Normalized healthy cell count and normalized healthy nuclear count of different concentrations (0.01 μM , 0.05 μM , 0.1 μM , 0.5 μM , 1 μM , 5 μM , 10 μM) of ricolinostat exposure with calculated IC50 values after 14h, 28h, 42h and 56h. **E** Normalized healthy cell count and normalized healthy nuclear count of different concentrations (0.01 μM , 0.05 μM , 0.1 μM , 0.5 μM , 1 μM , 5 μM , 10 μM) of milciclib exposure with calculated IC50 values after 14h, 28h, 42h and 56h. **F** Normalized healthy cell count and normalized healthy nuclear count of different concentrations (0.05 μM , 0.01 μM , 0.05 μM , 0.1 μM , 0.5 μM , 1 μM , 5 μM) of cisplatin exposure with calculated IC50 values after 14h, 28h, 42h and 56h. **G** Correlation between healthy cell count and healthy nuclei count after 14 h of compound exposure normalized to healthy cells exposed to DMSO 0,1% in U2OS cells. **H** Correlation between healthy cell count and healthy nuclei count after 42 h of compound exposure normalized to healthy cells exposed to DMSO 0,1% in U2OS cells. **I** Fractions of High Via gating and fractions of healthy, fragmented and pyknosed nuclei after exposure to different concentrations (0.01 μM , 0.05 μM , 0.1 μM , 0.5 μM , 1 μM , 5 μM , 10 μM) of JQ1, staurosporine or paclitaxel in U2OS cells after 56h (JQ1, staurosporine) or 72h (paclitaxel) of compound exposure.

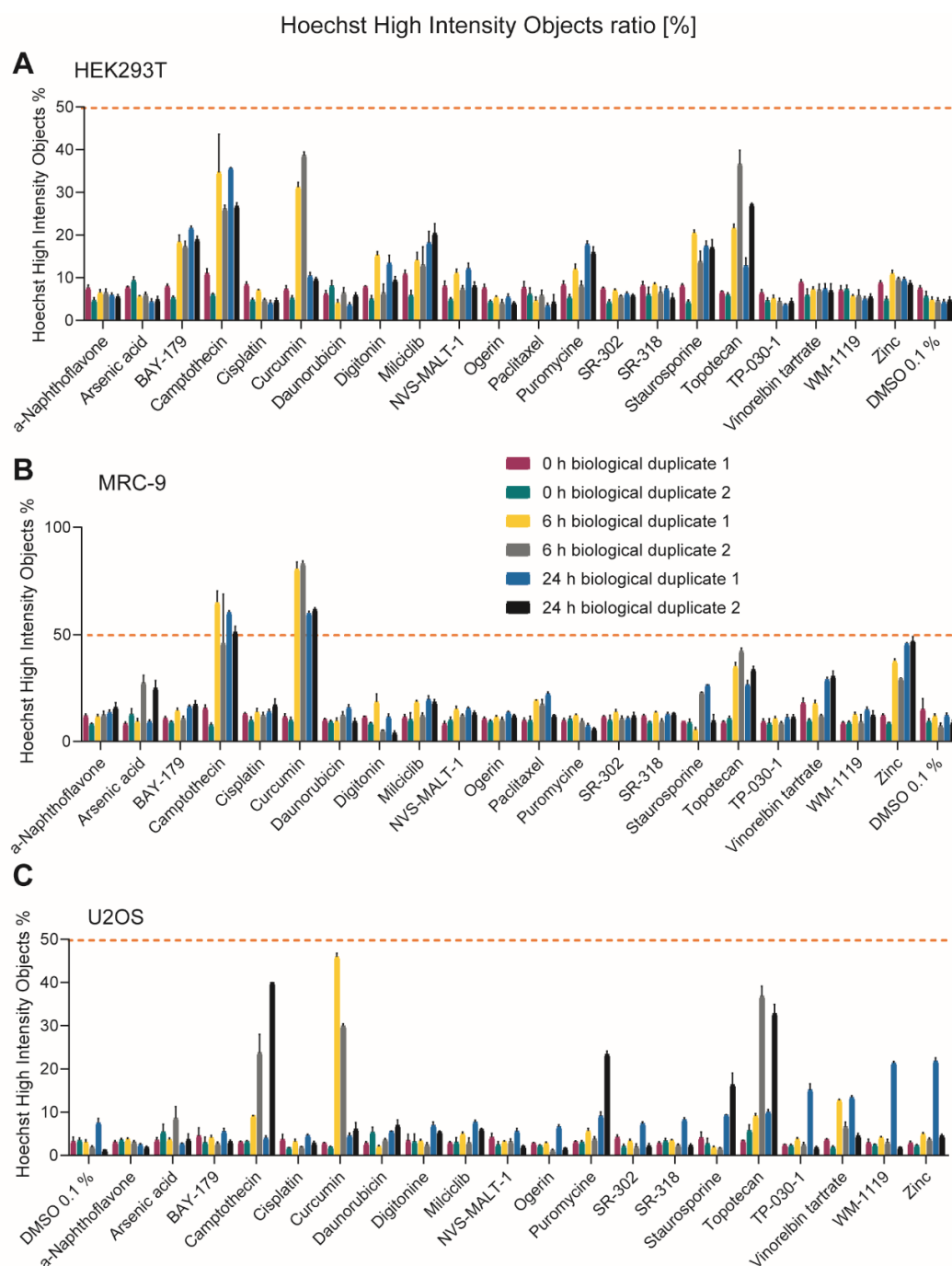


Supplementary Figure S3: Fluorescence Spectrum of Berzosertib **A** Fluorescence spectrum of Berzosertib 10 μ M in DMEM and DMEM alone at 311 nm and 340 nm. **B** Fluorescence spectrum of Berzosertib 10 μ M in EMEM and EMEM alone 311 nm and 340 nm



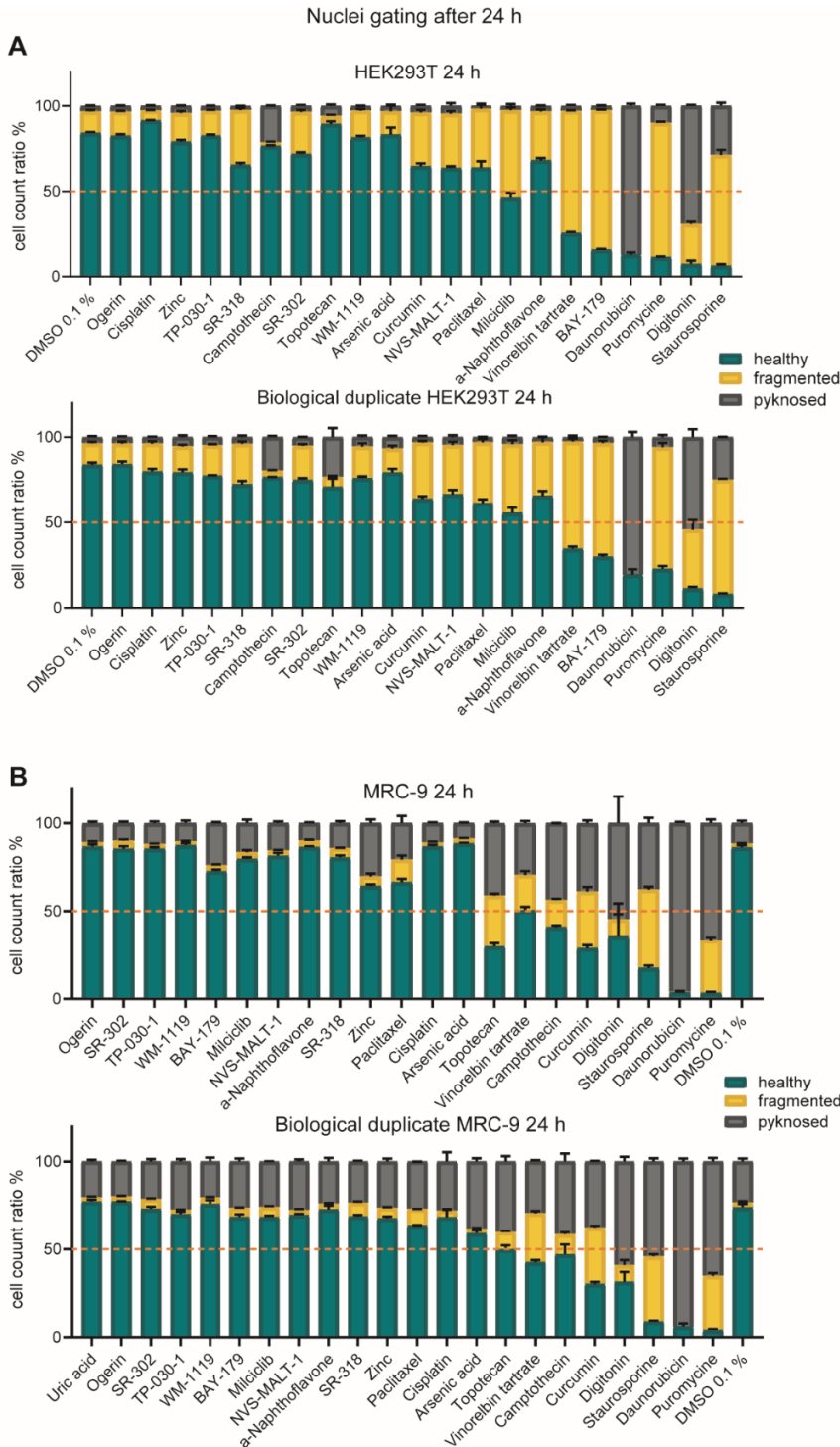
Supplementary Figure S4: Validation of Multiplex high Via protocol **A** Correlation of phenotypical analysis of tubulin mitochondrial mass increase of biological duplicates in U2OS cells after 24h. **B** Correlation of tubulin effect and pyknotic nuclei analysis in U2OS cells after 6

h (purple) and 24h (green). **C** General workflow of “old” analysis. **D** Correlation of “old” and “new” analysis of tubulin effect (purple) and mitochondrial mass (green) analysis in U2OS cells after 24h. **E** Cell count ratio of tubulin effect (orange) and mitochondrial mass increase (blue) of “old” and “new” analysis in U2OS cells after 24h of 10 μ M of compound exposure (Suppl. tabl.3) in comparison to DMSO 0.1%. Error bars show SEM of technical triplicates.



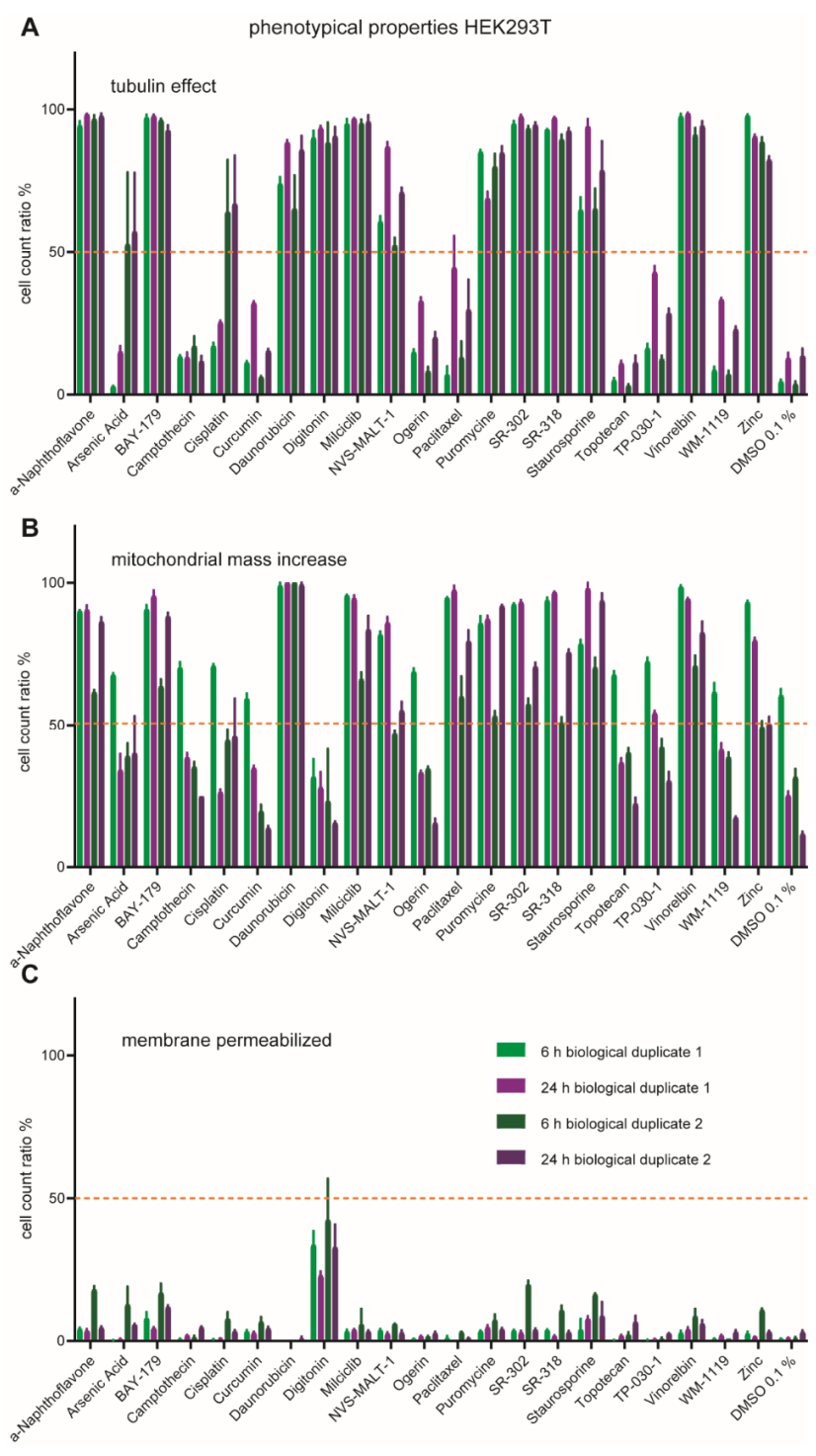
Supplementary Figure S5: Hoechst High Intensity Object Analysis. **A** Ratio of Hoechst High Intensity Objects after 0h, 6h and 24h of compound exposure (Supplementary Table S4) in HEK293T cells in comparison to DMSO 0.1% of biological duplicates. Error bars show SEM of technical triplicates. Property threshold at 50% marked red. **B** Ratio of Hoechst High Intensity Objects after 0h, 6h and 24h of compound exposure (Supplementary Table S4) in MRC-9 cells in

comparison to DMSO 0.1% of biological duplicates. Error bars show SEM of technical triplicates. Property threshold at 50% marked red. **C** Ratio of Hoechst High Intensity Objects after 0h, 6h and 24h of compound exposure (Supplementary Table S4) in MRC-9 cells in comparison to DMSO 0.1% of biological duplicates. Error bars show SEM of technical triplicates. Property threshold at 50% marked red.



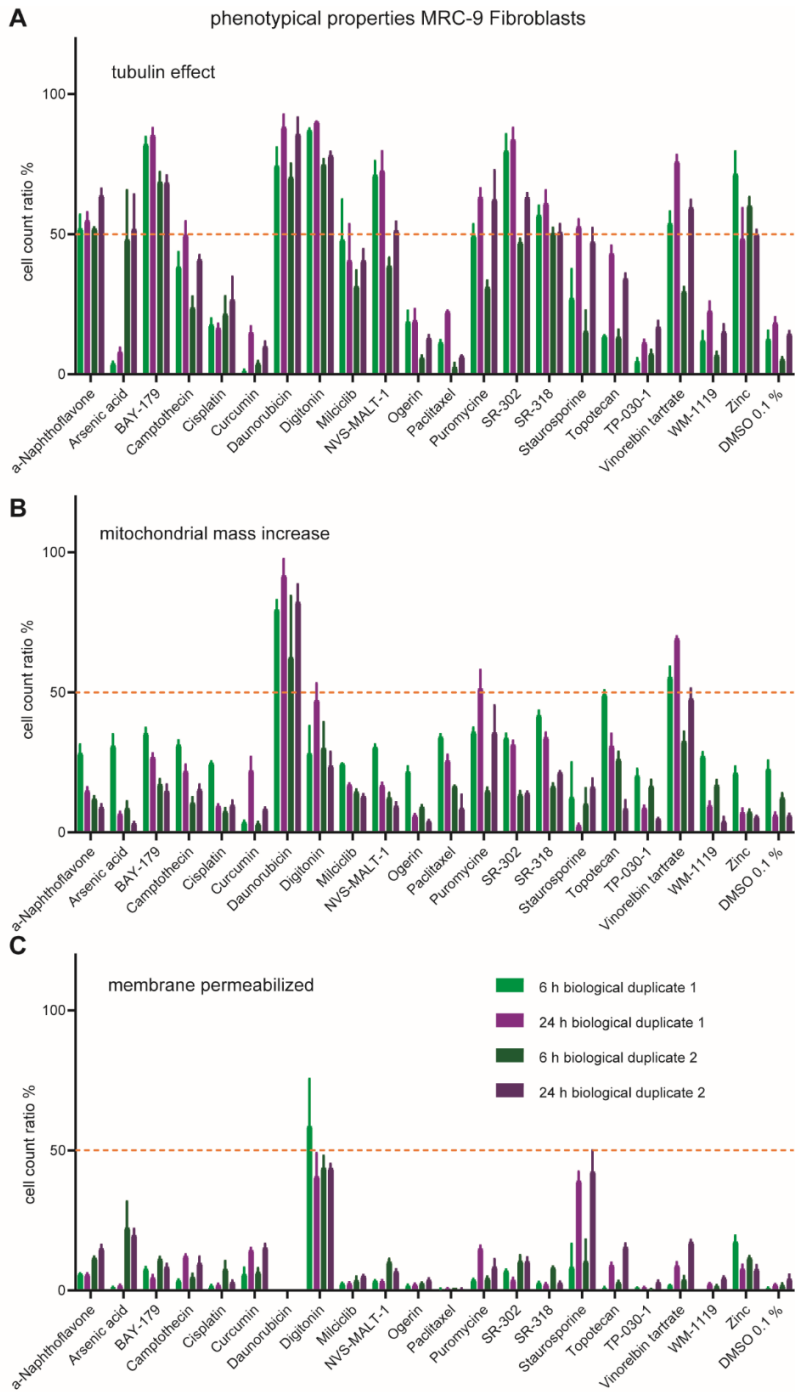
Supplementary Figure S6: Viability analysis over nuclei gating protocol A Cell count ratio of different Nuclei gating after 24h of 10 μ M of compound exposure (Supplementary Table S4) in comparison to DMSO 0.1% in HEK293T cells. Error bars show SEM of technical triplicates.

Property threshold at 50% marked red. Both biological duplicates are shown. **B** Cell count ratio of different Nuclei gating after 24h of 10 μ M of compound exposure (Supplementary Table S4) in comparison to DMSO 0.1% in MRC-9 cells. Error bars show SEM of technical triplicates. Property threshold at 50% marked red. Both biological duplicates are shown.

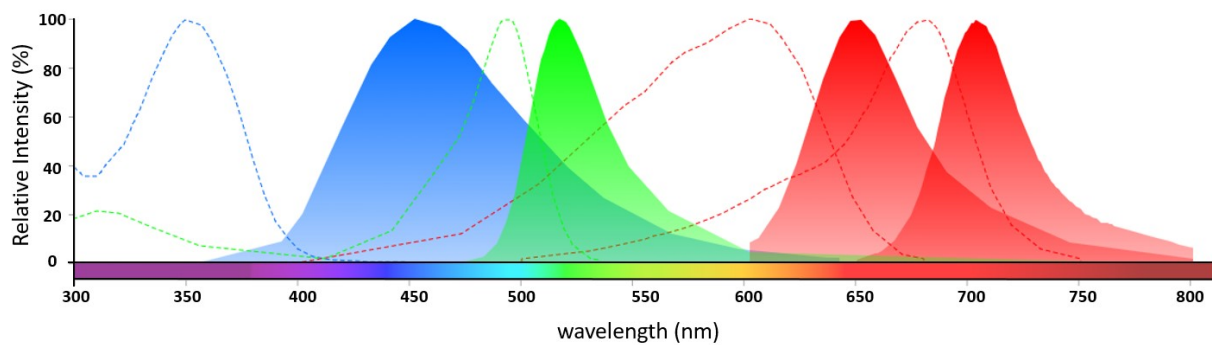


Supplementary Figure S7: Phenotypical property analysis in HEK293T cells. Cell count ratio of tubulin effect (S7 A), mitochondrial mass increase (S7 B) and membrane permeability (S7 C) of HEK293T cells after 6h and 24h of 10 μ M of compound exposure (Supplementary Table S4)

in comparison to DMSO 0.1%. Error bars show SEM of technical triplicates. Property threshold at 50% marked in red. Both biological replicates are shown.



Supplementary Figure S8: Phenotypical property analysis in MRC-9 cells. Cell count ratio of tubulin effect (S7 A), mitochondrial mass increase (S7 B) and membrane permeability (S7 C) of MRC-9 cells after 6h and 24h of 10 μ M of compound exposure (Supplementary Table S4) in comparison to DMSO 0.1%. Error bars show SEM of technical triplicates. Property threshold at 50% marked in red. Both biological replicates are shown.



Supplementary Figure S9: Spectra Viewer visualization. Spectra Viewer visualization of fluorophore excitation and emission wavelengths (<https://www.thermofisher.com/uk/en/home/life-science/cell-analysis/labeling-chemistry/fluorescence-spectraviewer.html>). Hoechst (blue), BioTracker™ 488 Green Microtubule Cytoskeleton Dye (green), MitoTracker red (Red) and Annexin V Alexa Fluor 680 conjugate (deep red), as used in the protocol.

Supplementary Table S1: Concentrations in μ M of tested cell staining dyes. Concentration used in described assays are marked in blue.

| number | Hoechst33342 | Yo-Pro-3 | BioTracker™ 488 Green Microtubule Cytoskeleton Dye | Mitotracker™ red | Mitotracker™ far red |
|--------|--------------|----------|--|------------------|----------------------|
| 1 | 0.02 | 0.1 | 1 | 0.01 | 0.01 |
| 2 | 0.035 | 0.5 | 2 | 0.05 | 0.05 |
| 3* | 0.060 | 1 | 3 | 0.075 | 0.075 |
| 4 | 0.085 | 3.5 | 4 | 0.1 | 0.1 |
| 5 | 0.130 | 5 | 5 | 0.5 | 0.5 |
| 6 | 0.170 | 10 | 6 | 1 | 1 |

* concentration used in Multiplex and High Via Extend protocol

Supplementary Table S2: reference compounds tested in High-Via Extend protocol

| Reference compound | Mode of action | Predominant cell death type | IC 50 14 h | IC 50 26 h | IC 50 42 h | IC 50 56 h |
|----------------------|---|--|------------|------------|------------|------------|
| digitonin | detergent | lysis | 10.6 | 11.6 | 11.5 | 15.1 |
| torin | mTOR kinase inhibitor | Apoptosis, autophagy | 0.8 | 0.8 | 0.7 | 0.7 |
| ricolinostat | HDAC 6 inhibitor | Apoptosis, cell cycle arrest | n/a | 13.5 | 13.4 | 13.7 |
| paclitaxel | targets tubulin/no disassembly of mitotic spindle | Apoptosis, tubulin binder, cell cycle arrest | > 2 | 0.1 | 0.06 | 0.05 |
| staurosporine | kinase inhibitor | Apoptosis | 0.005 | 0.004 | 0.003 | <0.001 |
| JQ1 | BET inhibitor | Apoptosis, cell cycle arrest | 9.7 | 9.0 | 13.7 | 0.2 |
| berzosertib | ATR/ATM-inhibitor | Apoptosis, DNA damage response | 62.7 | 64.1 | 58.7 | 56.5 |
| milciclib | CDK inhibitor | Apoptosis, cell cycle arrest | 2.1 | 0.8 | 0.6 | 0.5 |
| camptothecin | topoisomerase inhibitor | Apoptosis, DNA damage response | 2.6 | 2.3 | 1.5 | 1.1 |

Supplementary Table S3: Compounds tested in FUCCI Assay System

| compound | mode of action | concentration [μM] | known cell cycle effect | main nuclei color | reference |
|------------------|---|--------------------|--|-------------------|-----------|
| α-Naphthoflavone | flavone derivate, inhibitor of enzyme aromatase | 10 | G1 cell cycle arrest | red | [39,35] |
| Bromosporine | bromodomain (BET) inhibitor | 10 | increase of cells in G1 phase → cell cycle block | red | [74] |
| Camptothecin | topoisomerase inhibitor I | 10 | mitotic arrest | green | [27,75] |
| Daunorubicine | topoisomerase inhibitor II | 10 | DNA double strand breaks, cell cycle arrest | yellow | [47] |
| Doxorubicine | topoisomerase inhibitor II | 10 | G0/G1 cell cycle arrest after continuous treatment with 5 μM | yellow | [76] |

| | | | | | |
|---------------|---|----|---|--------|------------|
| HI-TOPK-032 | TOPK inhibitor | 10 | TOPK serine/threonine kinase is phosphorylated during mitosis, G1 cell cycle arrest | yellow | [48] |
| JH-XI-05-01 | SRPK1/2 inhibitor[1] | 10 | not described previously | red | [77] |
| Milciclib | CDK inhibitor | 10 | G1 cell cycle arrest | red | [37,38] |
| Mitoxantrone | topoisomerase inhibitor II | 10 | delay in cell cycle progression | green | [78,43,44] |
| Paclitaxel | targets tubulin/no disassembly of mitotic spindle | 10 | concentration-dependent G1 or Mitosis cell cycle arrest | red | [40,41] |
| Panobinostat | histone deacetylase (HDAC) inhibitor | 10 | G1/S cell cycle arrest | green | [79] |
| Puromycine | aminonucleoside antibiotic | 10 | effect on cell cycle checkpoints | red | [80] |
| Staurosporine | kinase inhibitor | 10 | dose-dependent cell cycle arrest in G1 or G2 | green | [81] |
| T3-CLK | CLK inhibitor | 10 | G2/M cell cycle arrest | green | [82] |

Supplementary Table S5: References used for Multiplex protocol

| compound | mode of action | concentration [μM] |
|-----------------|--|--------------------|
| Ogerin | positive allosteric modulator of GPR68 (DCP probe) | 10 |
| TP-030-1 | RIPK1 inhibitor (DCP probe) | 10 |
| WM-1119 | KAT6A, KAT6B inhibitor (DCP probe) | 10 |
| SR-302 | DDR1, DDR2, MAPK11, MAPK14 inhibitor (DCP probe) | 10 |
| NVS-MALT1 | MALT1 allosteric inhibitor (DCP probe) | 10 |
| Zinc | trace element, corrosive | 10 |
| Cisplatin | interfering in DNA replication | 10 |
| Arsenic acid | toxic and corrosive chemical compound | 10 |
| SR-318 | MAPK14 inhibitor (DCP probe) | 10 |
| α-Naphtoflavone | flavone derivate, inhibitor of enzyme aromatase | 10 |
| BAY-179 | complex I inhibitor (DCP probe) | 10 |
| Curcumin | natural product | 10 |
| Milciclib | CDK inhibitor | 10 |
| Paclitaxel | targets tubulin/no disassembly of mitotic spindle | 10 |
| Topotecan | topoisomerase inhibitor | 10 |
| Digitonin | detergent | 10 |
| Camptothecin | topoisomerase inhibitor | 10 |

| | | |
|----------------------|--|----|
| Vinorelbine tartrate | vinca alkaloid, antimicrotubule agent | 10 |
| Staurosporine | kinase inhibitor | 10 |
| Puromycine | aminonucleosid antibiotic | 10 |
| Daunorubicine | anthracycline antibiotic, intercalate of DNA strands, ROS production | 10 |

Supplementary Table S6: Trainings set. Compounds to train the machine learning algorithm for Multiplex protocol

| reference compound | mode of action | predominant cell death type |
|----------------------|-----------------------------------|------------------------------|
| digitonin | detergent | lysis |
| paclitaxel | tubulin binder, cell cycle arrest | apoptosis |
| staurosporine | kinase inhibitor | apoptosis |
| miliciclib | CDK inhibitor | apoptosis, cell cycle arrest |
| dms0 | solvent | healthy cells |

Supplementary Table S7: Features of machine learning algorithm

Table.1: features used for machine learning algorithm in healthy/early apoptotic/late apoptotic/lysed and necrotic cells

| cell region | feature* | cell region | feature* |
|-------------|--------------------|-------------|---------------------|
| Cellbody | Area | Nuclei | Area |
| Cellbody | Diameter | Nuclei | Diameter |
| Cellbody | Circumference | Nuclei | Circumference |
| Cellbody | Circularity | Nuclei | Circularity |
| Cellbody | Compactness | Nuclei | Compactness |
| Cellbody | Anisometry | Nuclei | Anisometry |
| Cellbody | mean intensity CH2 | Nuclei | total intensity CH1 |
| Cellbody | mean intensity CH3 | Nuclei | mean intensity CH1 |
| Cellbody | mean intensity CH4 | Nuclei | mean intensity CH3 |

| | | | |
|----------|-----------------|--------|-----------------|
| Cellbody | mean peak CH2 | Nuclei | total peak CH3 |
| Cellbody | mean peak CH4 | Nuclei | total ridge CH1 |
| Cellbody | mean hole CH2 | Nuclei | mean ridge CH1 |
| Cellbody | mean hole CH4 | Nuclei | mean ridge CH3 |
| Cellbody | mean ridge CH2 | | |
| Cellbody | mean valley CH2 | | |
| Cellbody | mean valley CH4 | | |
| Cellbody | mean edge CH4 | | |
| Cellbody | mean saddle CH2 | | |
| Cellbody | mean saddle CH4 | | |

Table 2: features used for machine learning algorithm in healthy/pyknosed and fragmented cell nuclei

| cell region | feature* | cell region | feature* |
|-------------|---------------------|-------------|-----------------|
| Nuclei | total intensity CH1 | Nuclei | mean ridge CH1 |
| Nuclei | total hole CH1 | Nuclei | mean valley CH1 |
| Nuclei | total valley CH1 | Nuclei | mean edge CH1 |
| Nuclei | total edge CH1 | Nuclei | mean saddle CH1 |
| Nuclei | total saddle CH1 | | |
| Nuclei | mean hole CH1 | | |

Table S3: features used for machine learning algorithm in High Intensity Objects and Normal Intensity Objects based

| cell region | feature* | cell region | feature* |
|-------------|--------------------|-------------|--|
| Cellbody | mean intensity CH1 | Nuclei | max intensity CH1 |
| Cellbody | min intensity CH1 | Nuclei | Nuc_cell_area Nuc Area / Cellbody Area |
| Cellbody | max intensity CH1 | | |

Table 4: features used for machine learning algorithm for Fucci assay in red/green and yellow nuclei

| cell region | feature* | cell region | feature* |
|--------------------|--------------------|--------------------|-----------------|
| Cellbody | mean intensity CH3 | Nuclei | total peak CH3 |
| Cellbody | mean peak CH2 | Nuclei | total edge CH2 |
| Cellbody | mean peak CH3 | Nuclei | total edge CH3 |
| Cellbody | mean hole CH2 | Nuclei | mean edge CH2 |
| Cellbody | mean hole CH3 | | |
| Cellbody | mean ridge CH2 | | |
| Cellbody | mean ridge CH3 | | |
| Cellbody | mean valley CH2 | | |
| Cellbody | mean valley CH3 | | |
| Cellbody | mean saddle CH2 | | |
| Cellbody | mean saddle CH3 | | |

Table 5: features used for machine learning algorithm in mitotic or apoptotic cells

| cell region | feature* | cell region | feature* |
|--------------------|---------------------|--------------------|-----------------|
| Cellbody | total intensity CH4 | Nuclei | total hole CH1 |
| Cellbody | max intensity CH4 | Nuclei | mean peak CH1 |
| Cellbody | mean peak CH4 | Nuclei | mean hole CH1 |
| Cellbody | mean hole CH4 | Nuclei | mean ridge CH1 |
| Cellbody | mean ridge CH4 | Nuclei | mean valley CH1 |
| Cellbody | mean valley CH4 | | |
| Cellbody | mean saddle CH4 | | |

Table 6: features used for machine learning algorithm in tubulin effect and no tubulin effect

| cell region | feature* | cell region | feature* |
|--------------------|---------------------|--------------------|-----------------|
| Cellbody | total intensity CH2 | Cellbody | mean peak CH2 |
| Cellbody | mean intensity CH2 | Cellbody | mean ridge CH2 |
| Cellbody | max intensity CH2 | Cellbody | mean edge CH2 |

Table 7: features used for machine learning algorithm in mitochondrial mass increased and mitochondrial mass normal

| cell region | feature* | cell region | feature* |
|-------------|---------------------|-------------|-----------------|
| Cellbody | total intensity CH3 | Cellbody | mean peak CH3 |
| Cellbody | mean intensity CH3 | Cellbody | mean hole CH3 |
| Cellbody | max intensity CH3 | Cellbody | mean ridge CH3 |
| Cellbody | total peak CH3 | Cellbody | mean valley CH3 |
| Cellbody | mean saddle CH3 | | |

Table 8: features used for machine learning algorithm in membrane permeabilized and membrane normal

| cell region | feature* | cell region | feature* |
|-------------|---------------------|-------------|-----------------|
| Cellbody | total intensity CH2 | Cellbody | mean hole CH2 |
| Cellbody | total intensity CH4 | Cellbody | mean hole CH3 |
| Cellbody | mean intensity CH2 | Cellbody | mean ridge CH2 |
| Cellbody | mean intensity CH3 | Cellbody | mean ridge CH3 |
| Cellbody | max intensity CH2 | Cellbody | mean ridge CH5 |
| Cellbody | mean peak CH2 | Cellbody | mean valley CH2 |
| Cellbody | mean peak CH3 | Cellbody | mean valley CH3 |
| Cellbody | mean peak CH5 | Nuclei | Compactness |
| Cellbody | mean edge CH2 | | |

*

CH1: Hoechst33342 (DNA detection): Ex 405 nm/Em 447/60 nm, 500ms, 50%

CH2: BioTracker™ 488 Green Microtubule Cytoskeleton Dye (tubulin stain): Ex 488/Em 525/50 nm, 50 ms, 40%

CH3: MitoTracker red (mitochondrial mass detection): Ex 561 nm/Em 617/73 nm, 100 ms, 40%

CH4: Annexin V (apoptosis marker): Ex 640 nm/Em 685/40, 50 ms, 20%

CH5: bright field: 300ms, 100% transmission